Al-Azhar University Civil Engineering Research Magazine (CERM)
Vol. (43) No. (4) October . 2021

Experimental Investigation on the Shear Behavior of Concrete Deep Beams with Additions Quartz, Steel Fiber, and Basalt Fiber

Gomaa A. ElKarim[1*], Prof. Dr. Mostafa A. Osman[2**], and Prof. Dr. Alaa G. sherif [2**]

[1*] Faculty of Engineering, Beni Sueif University, Egypt

[2**] Department of Structural Engineering, Faculty of Engineering in Materia, Helwan University, Egypt

[2**] Department of Structural Engineering, Faculty of Engineering in Materia, Helwan University, Egypt

ملخص البحث :

تم إجراء هذا البحث بهدف دراسة تأثير إضافة ألياف الحديد وألياف البازلت والكوارتز للخلطة الخرسانية وذلك علي سلوك الكمرات الخرسانية العميقة وذلك للحصول على المزيد من الخصائص المرغوبة ، وتحسين اداء العناصر الخرسانية لتحمل أحمال أكبر ولتعزيز أو تحويل السلوك الكلي إلى أكثر ليونة وقوة محسنة للخرسانة. تم اجراء الاختبارات المعملية في معمل الخرسانة – بقسم الهندسة المدنية – كلية الهندسة بالمطرية جامعة حلوان وتم اختبار اربعه كمرات ذات قطاع مستطيل بأبعاد (100*400*1000)مم (عرض*ارتفاع*طول). قد تم استخدام نسبه ثابته من جميع الإضافات السابقة وهي (1.50%)من حجم الخرسانة. العينة الأولي لا يوجد بها اى اضافات حيث يوجد. الثلاث كمرات الاخري بها تم اضافة ألياف الحديد وألياف البازلت والكوارتز الي الخلطة الخرسانية كإضافة داخليه فى الخلطة الخرسانية بنسبة وهى (1.5%) من حجم الخلطة الخرسانة . واستنتج من هذه الدراسة إلى أن استخدام الإضافات له تأثير ايجابي علي سلوك الكمرات العميقه ولكن ألياف الحديد بنسبة 1.5 ٪ من الحجم له التأثير الأعلى على سلوك الخرسانة المسلحة .

ABSTRACT:

The shear behavior of deep beams cast with ordinary and fibrous concrete were studied experimentally. The main parameters were the types and ratio of additions to the concrete mix used, whether basalt fiber, end hooked steel fiber, and quartz powder. There were 4 deep reinforced concrete beams cast. One of them were made of the concrete mix without any additions, other 3 were made of basalt fiber, end-hooked steel fiber, and quartz powder added to the concrete mix. All specimens had the same top, bottom, and vertical RFT. The experimental results show the ductile behavior of (RC) deep members characterized by diagonal splitting. Steel fiber deep beams exhibit higher strength than steel fiber or quartz powder deep beams. When the additions ratio is increased, the mid-span deflection is decreased at the same loads. Moreover, the addition of steel fiber has an impact on the values of vertical mid-span displacement of deep beams.

Keywords: Reinforcement concrete; deep beam; cracking load; shear capacity; basalt fiber; steel fiber; quartz powder.

1. Introduction

When the obvious shear span-to-depth ratio is less than 2.0, structural elements are defined to be deep beams [1-3]. High shear forces are required to build the flexural behavior of deep beams because of the limited shear span, which is sufficient to destroy the shear resistance mechanism before they reach their flexural capacity. Deep beams' shear capacity, therefore, is a critical consideration in their design. A compression strut transmits a large amount of load straight to the supports, according to the results of tests. International codes and standards, like as ACI 318 [5], incorporate the strut and tie model (SATM) for determining the shear capacity of RC deep beams. The SATM is too difficult for design professionals to use. It is also possible to use the strut and tie model (SATM) to analyses the behavior of deep beams [6-8].

2. Previous Research

Several experimental results have been reported on the shear behavior of RC deep beams [9–12]. Several methods were employed to examine the performance and failure mechanisms of deep reinforced concrete beams. The impact of concrete intensity, levels of shear span–depth and reinforcement, load plate, and other parameters on deep beams' shear capability was investigated based on research in reference [13-16]. Wu et al. [17] Fifteen shear tests have been conducted for lightweight deep beams reinforced concrete aggregates. The members' failure process and the applicable calculation models have been studied. Gao, 2002 and Zhao, 2003 studied how the shear performance of deep beams affected by the steel fiber content.

3. Experimental Work

3.1. Materials Characteristics

Two main reinforcements were used; mild steel for stirrups with grade 240/350 and high- tensile steel for top and bottom reinforcement in deep beams with grade 400/600. Table 1 shows the properties of the reinforcement. The coarse aggregate was 20 mm in maximum nominal size. The specific gravity and void ratio of the fine aggregate were 2.5 and 0.5, respectively. Tables 2 and 3 represent the grading of coarse aggregate and fine aggregate. Figure 1 a, b, and c reveals the different additions utilized in our study (chopped basalt fibers, end-hooked steel fibers, and quartz powder). The chopped basalt fiber was 12mm in length, the end-hooked steel fiber was purchased from the Nassar group (M.F.) in Qalboubieh, Egypt, 35 mm in length and 0.8 mm in diameter.

All (RC) deep beams were cast at the same day using normal weight concrete with a targeted 28-day compressive strength of 25 MPa. 6 concrete cubic (150 × 150 × 150 mm) were cast for each specimen and kept under the same environmental conditions and tested on the day of specimens testing.

Table 1. Tensile properties of the reinforcement

Bar designation	Steel type	Diameter (mm)	Area (mm2)	Yield strength (MPa)	Ultimate strength (MPa)
#8	M.S	8	50.3	240	350
#12	H.T. S	12	113	400	600
#16	H.T. S	12	113	400	600

Table 2. Sorting of the coarse aggregate.

Sieve Size(mm)	40	20	10	5	pan
%Passing	100	96	26	6	0

Table3. Grading of fine aggregate.

Sieve Size(mm)	10	5	2.5	1.25	0.63	0.31	0.16	pan
%Passing	100	98	94	90	75	26	4	0

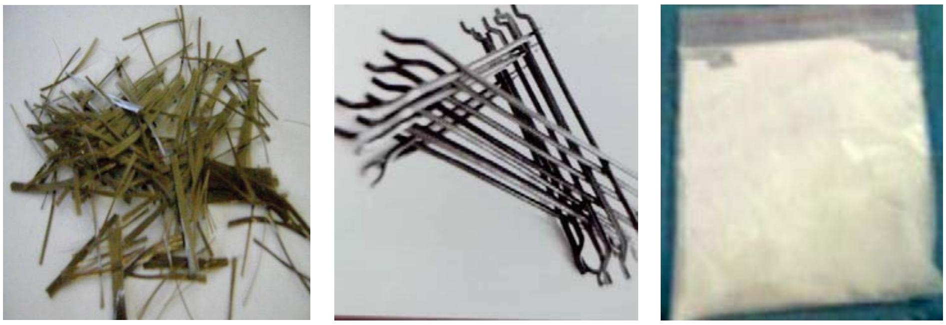

a) Basalt fiber b) End-hooked steel fiber c) quartz powder

Figure 1. Used Basalt fiber, end-hooked steel fiber and quartz powder.

3.2. Concrete Mix.

The proportions of these mixes are listed in Table 4. Sand, coarse aggregate, and amount of basalt/ steel fibers and quartz were added to the mechanical mixer and mixed for about one minute. Cement and the rest amount of the fibers were added without adding water for another one minute to ensure better dispersion of the fibers throughout the mix, then water is added gradually to the mixer and continued in mixing for about 5 minutes to obtain a homogenous mix for all constituents. It was observed that mixes with different fibers content were less workable than those without fibers, this may be due to the absorption of a certain amount of moisture by the fibers. Therefore, a super Plasticizer additive was added to the mix to enhance with 0.3 by water volume for enhancing the workability of the mix.

Table (4): Quantities by Weight for m^3 Concrete.

Mix No.	% Of steel fiber	Cement Content (kg/m^3)	Coarse Aggregates (kg/m^3)	Fine Aggregates (kg/m^3)	Addition type	Volume additions (kg/m^3)	Water (kg/m^3)
1	0.0%	350	1320	660	-----	0.0	175
2	1.5%	350	1320	660	Steel fiber	8.7	175
3	1.5%	350	1320	660	Basalt fiber	8.7	175
4	1.5%	350	1320	660	Quartz powder	8.7	175

3.3. Test Specimens

Experimental work consists of four deep beams, six cubes and six cylinders. The beams with dimensions 100 mm width, 400 mm height, 1000 mm length and 800 mm
Centre-right support to Centre-left support. The four beams classified into two groups as listed in Table 5. First group consists of one concrete beam without any additions to concrete mix, beam with 4Y16 bottom, 2Y12 top reinforcement and 5Φ8/m stirrups. The second group consists of three concrete beams with steel fiber, basalt fiber, quartz powder added to concrete mix with constant ratio equal to 1.50% from volume of concrete mix. Each of the three beams has the same top and bottom RFT, the reinforcements of beams are 4Y16 bottom RFT, 2Y12 top reinforcement, and 5Φ8/m stirrups Figure 2 shows the detail of specimen and locations of strain gauge and displacement gauge measuring points. All beams tested under two-point shear test.

Table (5): Specimens Details.

Beams	Bottom RFT	Top RFT	Stirrups	Fiber Ratio %
BC	4Y16	2Y12	5 ϕ 8/m	0
BS5	4Y16	2Y12	5 ϕ 8/m	1.50
BB5	4Y16	2Y12	5 ϕ 8/m	1.00
BQ5	4Y16	2Y12	5 ϕ 8/m	1.50

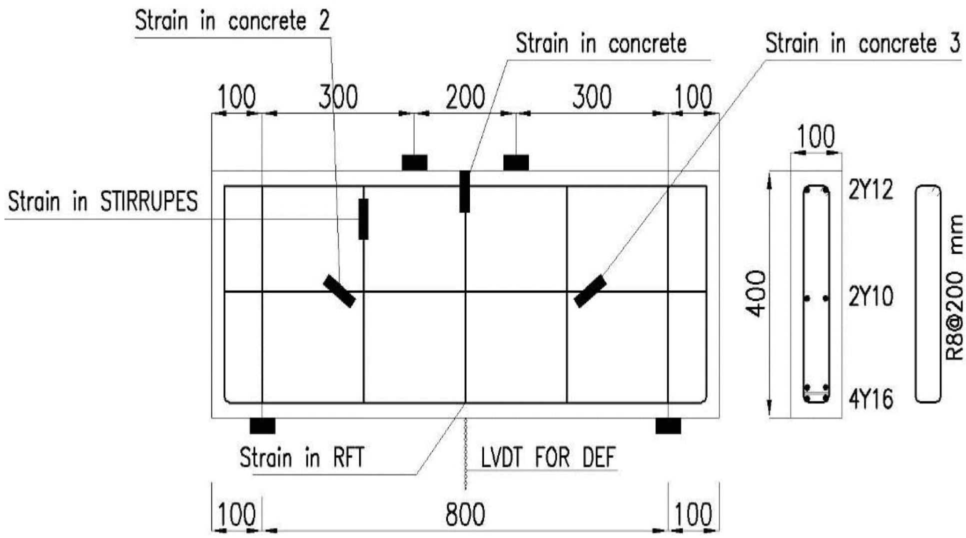

Figure 2. detail of tested deep beams.

3.4. TEST SETUP

Specimen setup is as shown in Figure.3, all specimens subjected to concentrated load using hydraulic jack at the middle of a distribution beam (I-sec). The distribution beam was supported on the tip of two bars that were fixed with the beam specimen at its ends.

Two LVDT for measuring deflections were located at mid span of the beam, 200 mm apart from support.

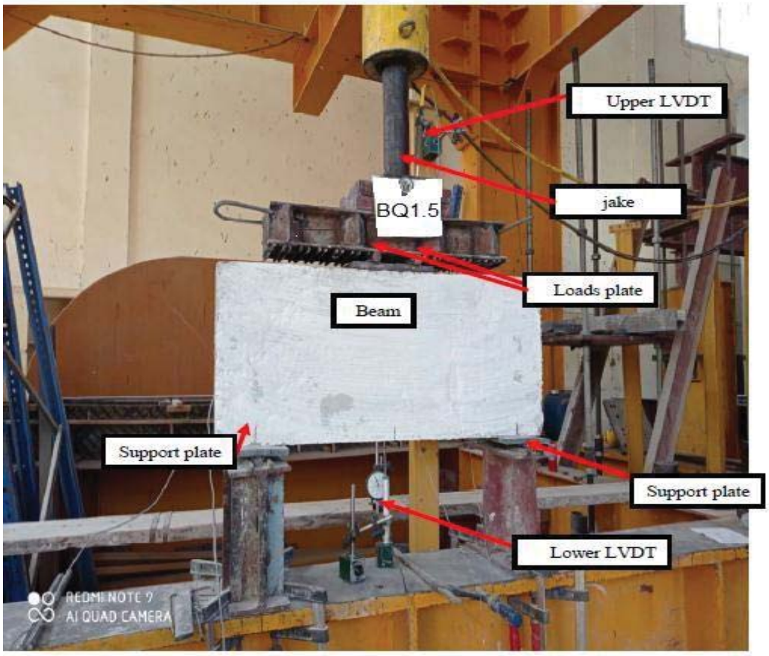

Figure. (3): Test setup of experimental work.

4. RESULTS OF EXPERMENTAL PROGREM

4.1. General Behavior and Cracking Patterns

As Figure 4, failure of all tested beams was only occurred after the first transverse crack entirely industrialized between the support plate and load. Meanwhile, direct diagonal crack, which like compression struts axis, was noted for all deep beams. It was noticed that the specimen with a steel fiber added to concrete mix diagonal crack in compression web is more than the one with quartz and/or basalt fiber. The final failure mode in this specimen experiment could be classified to only one type of failure pattern entitled failure by shear compression in the strut [18]. The compression strut failure was found in all deep beams (Figure 4). During the initial loading stage, diagonal cracks and flexural sequentially improved at the flexural shear portion and mid-span. The flexural cracks width is comparatively tiny, and hardly expanding after gently transmitted to 1/3–1/5 of the beam height along the upright route. All test samplings have various diagonal cracks equal to the connect line between the loading points and bearing, showing in figure 4. Finally, strut solidity failure was happened, mostly due to pounding the concrete among inclined cracks [18].

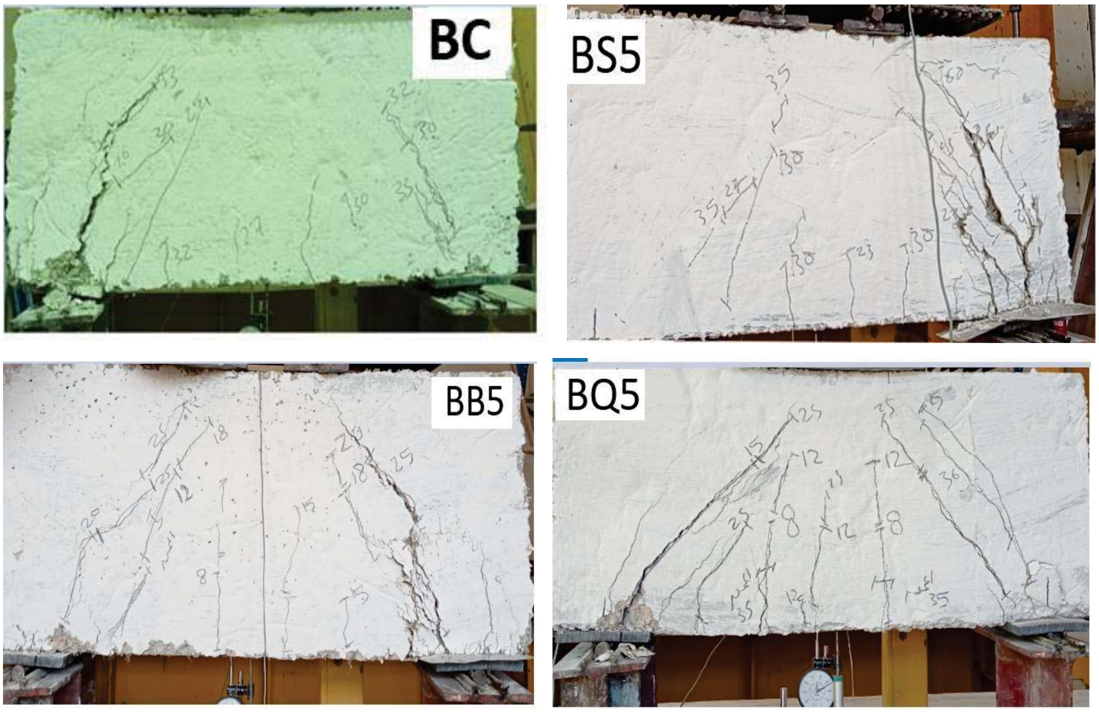

Figure 4. Failure mode for all specimen. Marked load(ton)

4.2. Failure Load

Figure 5 and table 6 shows the ultimate load for all specimens. Failure load for specimens is equal to beam (BC) was 400 KN, while maximum capacity load for beam (BS5) was 670 KN, maximum capacity load for beam (BB5) was 450 KN, and maximum capacity load for beam (BQ5) was 420 KN. By comparing results, it obvious that the steel fiber had high effect on deep beams than basalt fiber and quartz. Beam (BS5) increased by 67.50% of the controlled beam capacity, while beam (BB5) increased by 12.50 % of the controlled beam capacity and beam (BS3) increased by 5.00% of the controlled beam capacity of beam.

4.3. Crack Load to Failure Load Ratio

Figure 6 and Table 6 show the experimental crack load. Crack load to failure load ratio (BC) was 32.00 %; BS5 was 37 %; BB5 was 27.00 %; and BQ5 was 29.00 %. It was found that the crack load to failure load ratio of the BS5 beam increased by 2% when compared to BC, which indicates that steel fiber enhanced the section in order to reduce cracking. BC is more brittle than BB5 because BB2 reduced by 5.00% when compared to BC. When BQ5 was compared to BC, the difference was 3.00 percent, indicating that BC is more fragile. In order to get the best warning time before collapse, steel fiber should be used rather than basalt or quartz fibers.

Table 6: Results of Tested Specimens

Beam No.	Cracking Stage	Failure Stage		P_{cr}/P_u
	P_{cr} (KN)	P_u (KN)	δ at mid span (mm)	
BC	128	400	5	0.32
BS5	250	670	6.65	0.37
BB5	120	450	5.92	0.27
BQ5	120	420	3.51	0.29

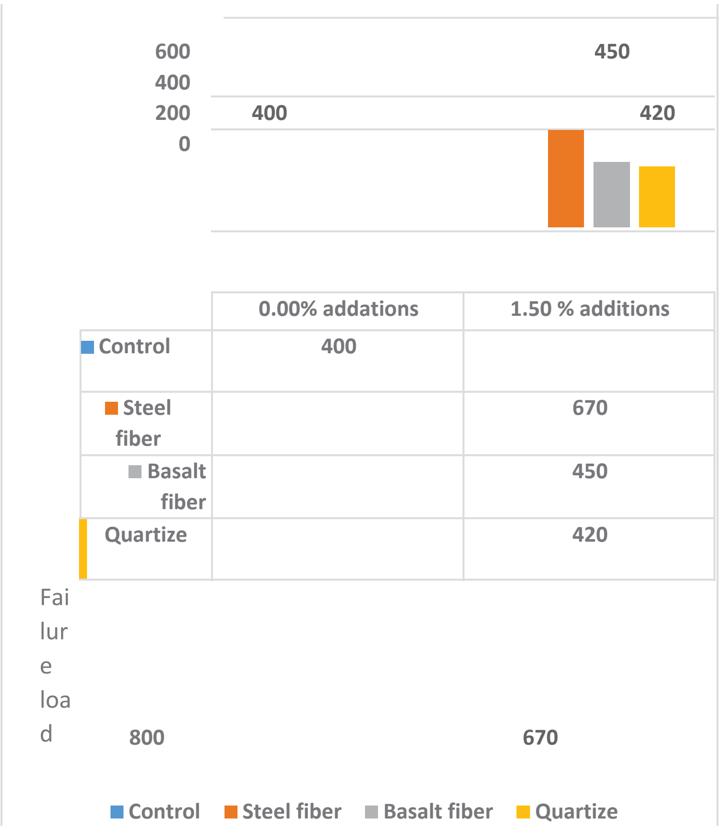

Figure 5: Failure Load for Specimens.

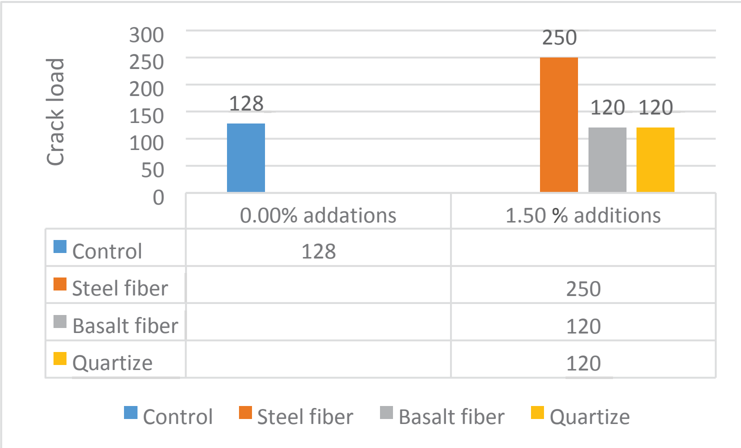

Figure 6: Crack Load for Specimens.

4.4. Load-Deflection Curves

The load-deflection charts from experimental work for all deep beams are presented in Figure 7. The response to load deflection is often well predicted. As shown in the figures, the sudden increase in deformation due to the formation of first flexural cracks can be detected. The figures show that increasing the amount of steel fiber, basalt fiber, and quartz powder leads to an increase in load-carrying capacity at various levels. The formation of the first diagonal crack reduced the beam stiffness significantly. All studied beams showed a certain ductility. The degree of ductility depended on the type and the ratio of additions. Figure (7) and Table 6 show the value of deflection at midspan for deep beams (BC, BS5, BB5, and BQ35). Moreover, for specimen BS5, the critical crack widened with the snapping of steel fibers. The bottom steel of all specimens are not yield. The vertical RFT are yield in all deep beams. Nonlinearity was seen in the mid-span load-deflection curves. After the maximum load, the mid-spanload deflection curves stayed at a constant level. Then, the loading of specimens was rejected slowly with an increase of mid-span vertical deflection. The ductile nature of load-midspan deflection curves was observed. The concrete could not bear the applied loading due to cracking in the filled concrete. Moreover, the stiffness of the specimens increased with an increase in the addition's ratio. Finally, tension failure of the specimens occurred.

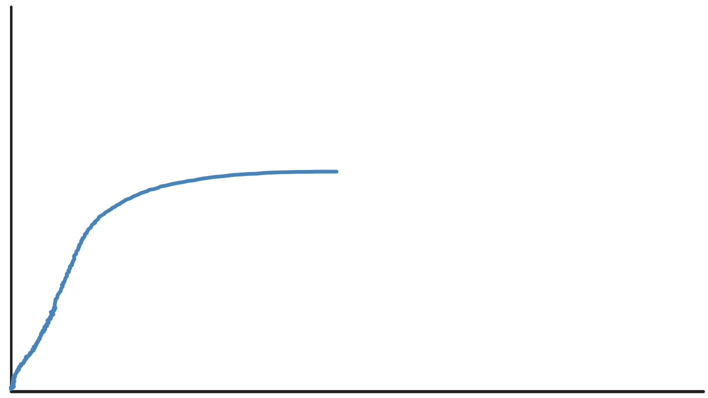

Fig. (7): Deflection at mid span for specimens (BC, BS1, BS2 and BS3)

5. CONCLUSION

1. Having steel fiber in mixture of tested beam with 1.5% percentage of volume made the beam carry a large amount of stress but didn't reach to the yield value of stress of steel.
2. Steel fiber in mixture improves the capacity of beams for deflection and failure load which had a higher failure load and minimum deflection at mid-span.
3. Having steel fiber in a mixture of the tested beams with 1.5% 3. percentage of volume made the stiffness of the beam better than beams with basalt or quartz additions.

6. REFRENCES :

1. ACI Committee 318. "Building Code Requirements for Structural Concrete and Commentary (ACI 318),". Farmington Hills, MI: American Concrete Institute; 2014. p. 503.

2. CSA A23.3. "Design of Concrete Structures Standard.". Mississauga, Ontario, Canada: Canadian Standards Association; 2014. p. 295.

3. Shahnewaz M, Rteil A, Alam M, S. "Shear strength of reinforced concrete deep beams – A review with improved model by genetic algorithm and reliability analysis.". Structures 2020; 23:494–508.

4. Yanga TY, Dashlejehb AA, Arabzadehc A, Hizajic R. "New model for prediction of ultimate load of prestressed RC deep beams.". Structures 2020; 23:509–17.

5. ACI Committee 318. Building code requirements for structural concrete (ACI 318-14). American Concrete Institute, Farmington Hills, MI, USA.; 2014.

6. Dashlejeh AA, Arabzadeh A. "Experimental and analytical study on RC deep beams". Int J Struct Eng 2019. https://doi.org/10.1504/IJSTRUCTE.2019.101408.

7. Arabzadeh A, Hizajic R, Yanga TY. "Experimentally studying and development of curved STM to predict the load capacity and failure mode of fixed-ended RC deep beams.". Structures 2020; 23:289–303.

8. Arabzadeh A. Analysis of boundary condition effects on RC deep beams. Structures 2020; 23:821–30.

9. Siess C. Strength and Behavior of Deep Beams in Shear. J Struct Div 1965; 91:19– 41.

10. Quintero-Febres CG, Parra-Montesinos G, Wight JK. Strength of struts in deep concrete members designed using strut-and-tie method. ACI Struct J 2006; 103:577–86.

11. Smith KN, Vantsiotis AS. Shear Strength of Deep Beams. J Am Concr Inst 1982; 79:201–13.

12. Wakjira T, Ebead U. Internal transverse reinforcement configuration effect of EB/NSE-FRCM shear strengthening of RC deep beams. Compos Part B Eng 2019; 166:758–72.

13. Liu L.Q., Wang, J.J., Han, J.Y., Zhang, G.X., Wu, X.L., "Experimental study on static performance of reinforced concrete simply-supported deep beams and analysis of compression rod model,". J. Build. Struct. 2013, 34, pp. 137–141, 2013.

14. Qiu, Y.K., Liu, X., Lin, Y. Experimental study on simply supported reinforced concrete deep beams of strut-and-tie models. Build. Struct. 2012, 42, 91–96.

15. Lu W. Y., Lin I. J., Yu H. W., "Shear strength of reinforced concrete deep beams,". ACI Structural journal, vol. 110, no. 4, pp. 671–680, 2013

16. Tan K. H., Cheng G. H., Zhang N., "Experiment to mitigate size effect on deep beams," Magazine of Concrete Research, vol. 60, no 10, pp. 709–723, 2008.

17. Wu T., Wei H., Liu X., "Shear behavior of large-scale deep beams with lightweightaggregate concrete," ACI Structural journal, vol 117, no 1, pp.75-89, 2020.

18. Nadesan M. S., Dinakar P., "Structural concrete using sintered flyash lightweight aggregate: A review," Construction and Building Materials, vol. 154, pp. 928-944, 2017.